Journal of Medicinal Plants Research Vol. 6(21), pp. 3694-3704, 9 June, 2012
Available online at http://www.academicjournals.org/JMPR
DOI: 10.5897/JMPR11.170
ISSN 1996-0875 ©2012 Academic Journals

Full Length Research Paper

Purple sweet potato color attenuates D-galactose-induced renal injury in mice by inhibiting the expression of NF-κB-dependent inflammatory genes

Shao-hua Fan[1#], Zi-feng Zhang[1#], Yan-yan Wang[2#], Yuan-lin Zheng[1]*, Jun Lu[1], Dong-mei Wu[1], Qun Shan[1] and Bin Hu[1]

[1]Key Laboratory for Biotechnology on Medicinal Plants of Jiangsu Province, School of Life Science, Xuzhou Normal University, Xuzhou 221116, P.R. China.
[2]First Renmin Hospital of Xuzhou, Xuzhou 221002, P.R. China.

Accepted 1 February, 2012

This study was carried out to investigate the protective effect of purple sweet potato color (PSPC) against D-galactose (D-gal)-induced renal injury and the possible mechanisms in mice. Histopathological analysis showed PSPC could significantly attenuate renal injury induced by D-gal. We found the protective effect of PSPC against D-gal induced renal injury might be caused, at least in part, by renewing the activity of antioxidant enzymes with a reduction in lipid peroxidation. These results implied that PSPC had a potential antioxidative activity. Furthermore, we found that PSPC had anti-inflammatory effects by reducing the expression of iNOS, COX-2, NF-κB p65, TNF-α, IL-1β, IL-6 and by decreasing the production of NO in D-gal-treated mice. Our findings suggested PSPC could attenuate renal injury induced by D-gal probably through its antioxidant and anti-inflammation properties. This study provided novel insights into the mechanisms of PSPC in the protection of the kidney.

Key words: Purple sweet potato color, D-galactose, antioxidant enzymes, NF-κB, proinflammatory cytokines.

INTRODUCTION

Anthocyanins are a class of naturally occurring polyphenol compounds that are responsible for the colors in most flowers and fruits of the higher plants (Wu et al., 2008). Interest in anthocyanin-rich food and extracts has intensified firstly due to their promising applications in the food industry as natural colorants. They can serve as alternatives to synthetic dyes in response to both legislative action and consumer concerns over the use of synthetic additives (Qiu et al., 2009). These anthocyanins not only have high stability but also have many beneficial effects, such as anti-oxidative (Piccolella et al., 2008; Peteros and Uy, 2010), anti-inflammatory (Mulabagal et al., 2009), anti-tumor properties (Shih et al., 2005). Recently, purple sweet potato (*Ipomoea batatas*) has aroused extensive attention because of its unique color, nutrition and its role in health care (Sakatani et al., 2007; Miyazaki et al., 2008; Choi et al., 2009). Purple sweet potato color (PSPC) is an abundant anthocyanin in the tuber of the Okinawa purple sweet potato, and these anthocyanins were already isolated and identified (Qiu et al., 2009). Many authors demonstrated that PSPC exhibited multiple physiological functions, such as antimutagenicity (Yoshimoto et al., 2001) and antihyper-

*Corresponding author. E-mail: ylzheng@xznu.edu.cn, yzheng170@yahoo.com.cn. Tel: +86 516 83500348. Fax: +86 516 83500348.

#These authors contributed equally to this work.

Abbreviation: PSPC, Purple sweet potato color; **Ctrl,** control; **D-gal,** D-galactose; **H&E,** hematoxylin and eosin; **MDA,** malondialdehyde; **SOD,** superoxide dismutases; **CAT,** catalase; **GPx,** glutathione peroxidase; **NO,** nitric oxide; **iNOS,** inducible nitric oxide synthase; **COX-2,** cylooxygenase-2; **NF-κB,** nuclear factor-kappa B; **TNF-α,** tumor necrosis factor-alpha; **IL-1β,** interleukin-1 beta; **IL-6,** interleukin-6.

glycemic effect (Matsui et al., 2002). D-galactose (D-gal) is a normal substance in the body, however, at high levels, it can cause the accumulation of reactive oxygen species (ROS), or stimulate free radical production indirectly by the formation of advanced glycation end products (AGEs) *in vivo*, finally resulting in oxidative stress (Zhang et al., 2005; Hua et al., 2007).

Mice injected with D-gal have been used as an animal model of oxidative damage (Lu et al., 2007). Recently, we also found in the mouse model, oxidative damage associated with inflammatory damage (Fan et al., 2009).

Kidney is an important urinary organ in our body, and maintaining proper kidney function is essential to keep us healthy. Research showed that renal injury could be induced by injection of D-gal into normal mouse (Li et al., 2005; Fan et al., 2009). However, to our knowledge, it has not yet been reported whether PSPC could attenuate the renal injury in D-gal-treated mice. Hence, the aim of the present study was to investigate whether PSPC has protective effect against D-gal-induced renal injury and, if so, by what mechanism.

MATERIALS AND METHODS

Animals

Eight-week-old male Kunming Strain mice (28.47 ± 5.43 g) were purchased from the Branch of National Breeder Center of Rodents (Shanghai). Prior to experiments mice had free access to food and water and were kept under constant conditions of temperature (23 ± 1°C) and humidity (60%). Ten mice were housed per cage on a 12-h light/dark schedule (lights on 08:30 to 20:30).

Experimental design

After acclimatization to the laboratory for 1 week, mice were divided randomly into four groups, termed as group A, group B, group C and group D. Mice in group B and group C received daily subcutaneous injection of D-gal (Sigma-Aldrich, MO, USA) at dose of 500 mg/kg/day for 8 weeks, and mice in group A and group D were injected with saline (0.9% NaCl). Then mice in group C and group D received purple sweet potato color (PSPC; purity > 90%; Qingdao Pengyuan Natural Pigment Research Institute) of 100 mg/kg/day in distilled water containing 0.1% Tween-80 (dH_2O/0.1% Tween-80) by oral gavage for another 4 weeks. Meanwhile, mice in group B and group A were given dH_2O/0.1% Tween-80 without PSPC. All experiments were performed in compliance with the Chinese legislation on the use and care of laboratory animals and were approved by the respective university committees for animal experiments.

Histological analysis

The mice were deeply anesthetized with sodium pentobarbital and perfused transcardially with 25 ml of normal saline (0.9%). The kidney tissues were fixed in a fresh solution of 4% paraformaldehyde (pH 7.4) at 4°C for 4 h, incubated overnight at 4°C in 100 mM sodium phosphate buffer (pH 7.4) containing 30% sucrose, and embedded in Optimal Cutting Temperature (OCT, Leica, CA, Germany). Cryosections (12 µm) were collected on 3-aminopropyl-trimethoxysilane-coated slides (Sigma-Aldrich).

Sections were stained with hematoxylin and eosin (H&E) and examined under light microscopy (Axioskop 40, Zeiss, Germany) by a board-certified veterinary pathologist who was blind to the animals assigned to each experimental group.

Tissue homogenates

For biochemical studies, animals were deeply anesthetized and sacrificed. Kidneys were promptly dissected and perfused with 50 mM (pH 7.4) ice-cold phosphate buffered saline solution (PBS). Kidneys were homogenized in 1/5 (w/v) PBS containing a protease inhibitor cocktail (Sigma-Aldrich, MO, USA) with 10 strokes at 1200 rev/min in a Potter homogenizer. Homogenates were divided into two portions and one part was directly centrifuged at 8000 ×g for 10 min to obtain the supernatant. Supernatant aliquots were used to determine kidney CAT, GPx activities, MDA levels and protein contents. The second part of homogenates was sonicated four times for 30 s with 20 s intervals using a VWR Bronson Scientific sonicator, centrifuged at 5000 ×g for 10 min at 4°C, and the supernatant was collected and stored at -70°C for determination of cytosolic Cu/Zn superoxide dismutase (SOD-1) enzyme activities. Protein contents were determined by using the BCA assay kit (Pierce Biotechnology Inc., Rockford, IL).

Measurement of malondialdehyde (MDA) level

Chemicals, including *n*-Butanol, thiobarbutiric acid, 1,1,3,3-tetramethoxy-propane and all other reagents, were purchased from Sigma Chemical Company. The level of MDA in kidney tissue homogenates was determined using the method of Mihara and Uchiyama (1978). Half a milliliter (0.5 ml) of homogenate was mixed with 3 ml of H_3PO_4 solution (1%, v/v) followed by addition of 1 ml of thiobarbituric acid solution (0.67%, w/v). Then the mixture was heated in a water bath at 95°C for 45 min. The colored complex was extracted into *n*-butanol, and the absorption at 532 nm was measured using tetramethoxypropane as standard. MDA levels were expressed as nmol per mg of protein.

Assay of Cu/Zn SOD activity

Chemicals used in the assay, including xanthine, xanthine oxidase, cytochrome *c*, bovine serum albumine (BSA) and SOD, were purchased from Sigma Chemical Company. SOD activity was measured according to the method described by Lu et al. (2005). Solution A was prepared by mixing 100 ml of 50 mM PBS (pH 7.4) containing 0.1 mM EDTA and 2 µmol of cytochrome *c* with 10 ml of 0.001 N NaOH solution containing 5 µmol of xanthine. Solution B contained 0.2 U xanthine oxidase/ml and 0.1 mM EDTA. 50 µl of a tissue supernatant was mixed with 2.9 ml of solution A and the reaction was started by adding 50 µl of solution B. Change in absorbance at 550 nm was monitored. A blank was run by substituting 50 µl of ultra pure water for the supernatant. SOD levels were expressed as U/mg protein with reference to the activity of a standard curve of bovine Cu/Zn SOD under the same conditions.

Assay of CAT activity

CAT activity was assayed by the method of Aebi (1984). In brief, to a quartz cuvette, 0.65 ml of the phosphate buffer (50 mmol/l; pH 7.0) and 50 µl sample were added, and the reaction was started by addition of 0.3 ml of 30 mM hydrogen peroxide (H_2O_2). The decomposition of H_2O_2 was monitored at 240 nm at 25°C CAT activity was calculated as nM H_2O_2 consumed/min/mg of tissue

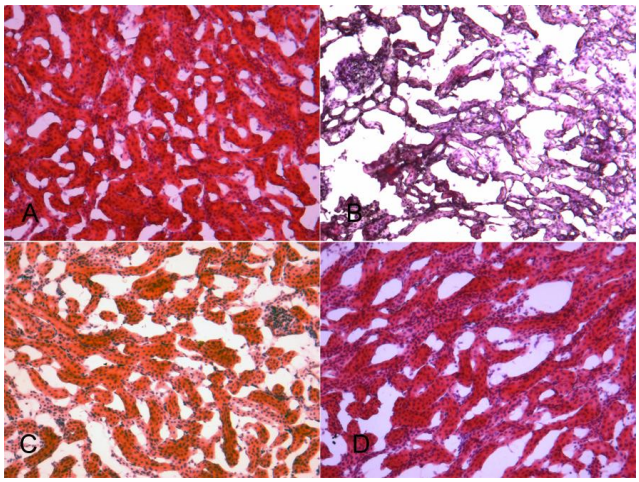

Figure 1. Hematoxylin and eosin-stained kidneys from the treated mice. (A) The vehicle control mice; (B) D-gal-treated mice; (C) D-gal-treated mice fed with PSPC and (D) PSPC-fed mice. Original magnification, 100×.

protein.

Assay of GPx activity

The GPx activity assay was based on the method of Paglia and Valentine (1967). Tert-butylhydroperoxide was used as substrate. The assay measures the enzymatic reduction of H_2O_2 by GPx through consumption of reduced glutathione (GSH) that is restored from oxidized glutathione GSSG in a coupled enzymatic reaction by GR. GR reduced GSSG to GSH using NADPH as a reducing agent. The decrease in absorbance at 340 nm due to NADPH consumption was measured in a Molecular Devices M2 plate reader (Molecular Devices, Menlo. Park, CA). GPx activity was computed using the molar extinction coefficient of 6.22 $mM^{-1}cm^{-1}$. One unit of GPx was defined as the amount of enzyme that catalyzed the oxidation of 1.0 µmol of NADPH to $NADP^+$ per minute at 25°C.

Measurement of NO level

NO was determined by measuring the accumulation of its stable oxidative metabolite, nitrite and nitrate using the standard colorimetric assay kit (Jiancheng Ltd, Nanjing, China). Briefly, the supernatant of homogenate was collected by a low-speed centrifugation. The samples were incubated at 37°C for 15 min in the presence of 0.1 U/ml nitrate reductase for converting nitrate to nitrite. After nitrate reduction, total nitrite of individual sample was determined spectrophotometrically by the Griess reaction. The concentration (µmol/L) of NO was evaluated according to the formula described in the manufacturer's instruction.

Protein and western blot analysis

Total protein extracts were prepared in 3 ml of ice cold RIPA lysis buffer (1×TBS, 1% NP-40, 0.5% sodium deoxycholate, 0.1% SDS, 0.004% sodium azide) combining 30 µl of 10 mg/ml PMSF solution, 30 µl of Na_3VO_4 and 30 µl of protease inhibitors cocktail per gram of tissue. Lysates were centrifuged at 10,000 ×g for 10 min at 4°C, and then remove the supernatants and centrifuge again. The supernatants were collected. Protein content in the supernatants was determined by using the BCA protein assay (Pierce Biotechnology, Inc., Rockford, IL, USA). Equal amounts of protein (40 to 60 µg) were loaded per lane onto SDS-PAGE gel. Proteins were transferred to a PVDF membrane (Roche Diagnostics Corporation, Indianapolis, IN, USA) by electrophoretic transfer. The membrane was pre-blocked with 5% non-fat milk and 0.1% Tween-20 in Tris-buffered saline (TBST), incubated overnight with specific primary antibodies for NF-κB, TNF-α, IL-1β, IL-6 (all them from Santa Cruz Biotechnology, CA, California, USA), COX-2 (Cell Signaling Technology, Beverly, MA, USA) and iNOS (BD, San Jose, CA, USA). Each membrane was washed three times for 15 min and incubated with the secondary horseradish perocidase-linked antibodies (Santa Cruz Biotechnology, CA and Cell Signaling Technology, Beverly, MA, respectively). Quantitation of detected bands was performed with the Scion Image analysis software (Scion Corp., Frederick, MD, USA). To prove equal loading, the blots were analysed for β-actin expression using an anti-β-actin antibody (Chemicon International Inc., Temecula, CA). Each density was normalized using each corresponding β-actin density as an internal control and averaged from the samples, and we standardized the density of vehicle control for relative comparison as 1.0 to compare with other groups.

Statistic analysis

All statistical analyses were performed using the SPSS software, version 11.5. Analysis of variance (ANOVA) was carried out with Newman-Keuls or Tukey's HSD post hoc test for multiple comparisons. Data were expressed as means ± S.E.M. Statistical significance was set at $p < 0.05$.

RESULTS

Histological studies on effects of PSPC in the D-gal-treated mice kidneys

Compared with the control group (Figure 1A), the kidneys from the D-gal group mice (Figure 1B) had severe tubular necrosis with vacuolization in proximal tubules and cast formation. The histological changes in the D-gal group included degeneration of tubular architecture, tubular dilation, proteinaceous debris, swelling, necrosis and luminal congestion with loss of brush border. Compared to the control groups, D-gal resulted in increased collagen in the glomeruli and around the tubules. In contrast, intriguingly, the kidneys from the D-gal + PSPC group mice (Figure 1C) showed much less damage. Tubular dilation, vacuolization of proximal tubules and cast formation were still observed but were much less marked than that in the D-gal groups. In addition, compared with normal mice, there were no visible histological changes in the kidneys of the mice treated with PSPC only (Figure 1D).

Effects of PSPC on lipid peroxidation in D-gal-treated mice kidneys

Lipid peroxide is a well-established mechanism of cellular injury, and is used an indicator of oxidative stress in cells and tissues. MDA, lipid peroxide derived from poly-

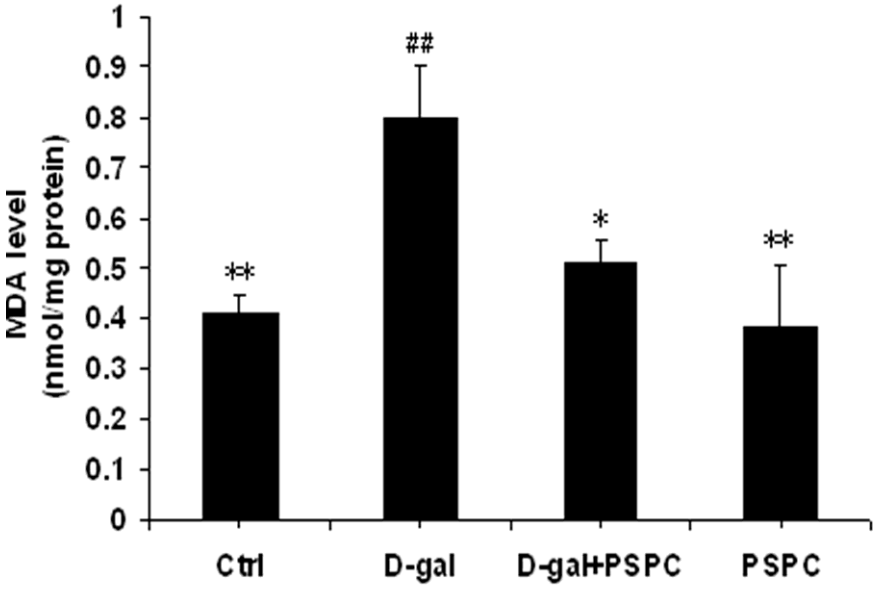

Figure 2. The effects of PSPC on the changes of MDA level induced by D-gal in the kidneys of mice. Each value is the means ± S.E.M. (n = 3). *P < 0.05; **P < 0.01, as compared to the D-gal model; # #P<0.01, as compared to the control group.

unsaturated fatty acids, is widely employer as an indicator of oxidative stress as well as lipid peroxidation because it is more abundant than other reactive carbonyl compounds (Kim et al., 2009). Figure 2 shows that PSPC could decrease D-gal induced lipid peroxidation level. D-gal-treatment caused significant increase by 96.3% in renal level of MDA as compared with vehicle controls (P < 0.01). The increase in lipid peroxidation indicates an elevated *in vivo* oxidative stress in the kidney of D-gal-treated mice. Interestingly, the renal MDA content of the mice treated with PSPC after D-gal injection was significant reduced by 35.8% as compared with D-gal-treated mice (P < 0.05). There was no significant difference with regard to the MDA content between PSPC-fed mice and the vehicle controls.

Effects of PSPC on antioxidative status of D-gal-treated mice kidneys

Biochemical antioxidants and a host of enzymic reactions supply the necessary reduction potential to maintain cells in a state of redox balance. Figure 3 presents the effect of PSPC on the activities of Cu/Zn SOD, CAT and GPx in the kidney of normal and D-gal-treated mice. The depletion of Cu/Zn SOD, CAT and GPx activities in kidney is a sign of indirect generation of free radicals. In D-gal-treated mice, Cu/Zn SOD (P < 0.001), CAT (P < 0.05) and GPx (P < 0.01) activities decreased significantly by 41.3, 48.5 and 74.0% as compared with those in the vehicle controls, respectively. PSPC treatment produced significant effect on these enzymic antioxidants in D-gal-treated mice and increased their activities by 0.4, 1.0 and 2.1-fold when compared with D-gal alone treated mice (Cu/Zn SOD: P < 0.05; CAT: P < 0.05; GPx: P < 0.05).

Effects of PSPC on NO production in D-gal-treated mice kidneys

Since NO is known to be a pro-inflammatory mediator in many different acute and chronic inflammatory diseases, we next addressed whether PSPC modulated NO production activated by D-gal. The results showed that the secretion of NO was significantly increased by 3.3-fold in the D-gal only-treated group as compared with those in the vehicle controls (P < 0.001). As shown in Figure 4, PSPC treatment produced significant effect in D-gal-treated mice and significantly decreased the secretion of NO by 12.7% than that with single D-gal stimulation (P < 0.01). There was no significant difference with regard to the NO content between PSPC-fed mice and the vehicle controls.

Effects of PSPC on the expression of iNOS, COX-2 and NF-κB p65 in the kidneys of D-gal-treated mice

To investigate whether the inhibitory effect PSPC on NO production was via inhibition of corresponding gene expression, the protein expression of iNOS were determined by Western blot analysis. Additionally, the COX-2 expression was also detected in this study. As

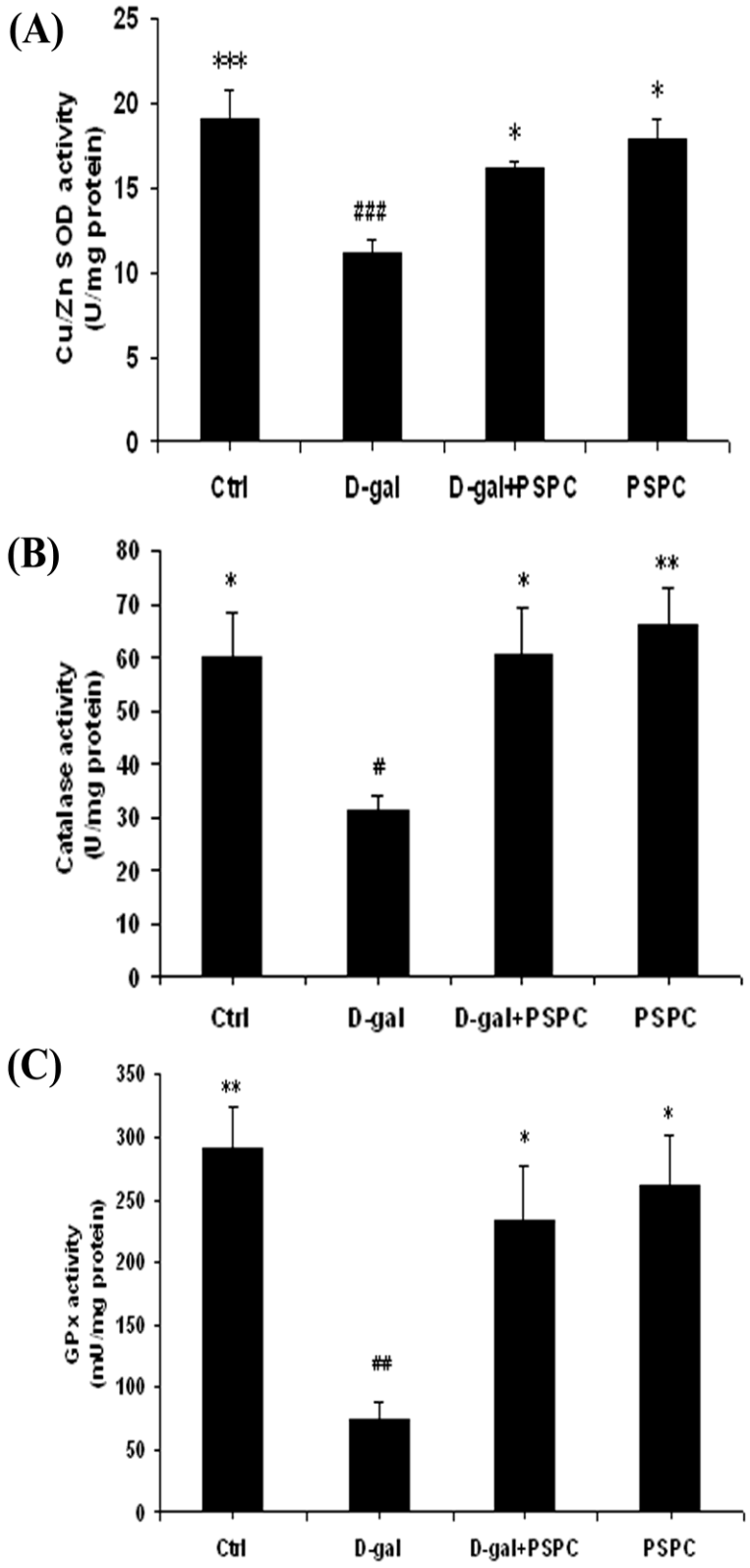

Figure 3. The effects of PSPC on the activity changes of Cu/Zn SOD, (A) CAT; (B) GPx; (C) induced by D-gal in the kidneys of mice. Each value is the means ± S.E.M. (n = 3). *P < 0.05; **P < 0.01; *** P<0.001, as compared to the D-gal model; #P < 0.05; ##P<0.01; ###P < 0.001, as compared to the control group.

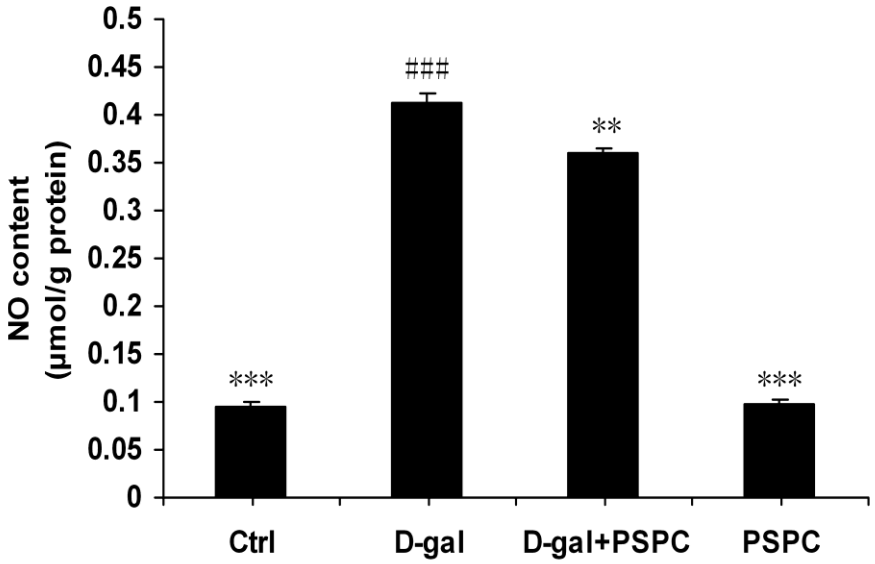

Figure 4. The effects of PSPC on the changes of NO content induced by D-gal in the kidneys of mice. Each value is the means ± S.E.M. (n = 3). **P < 0.01; ***P < 0.001, as compared to the D-gal model; # # #P < 0.001, as compared to the control group.

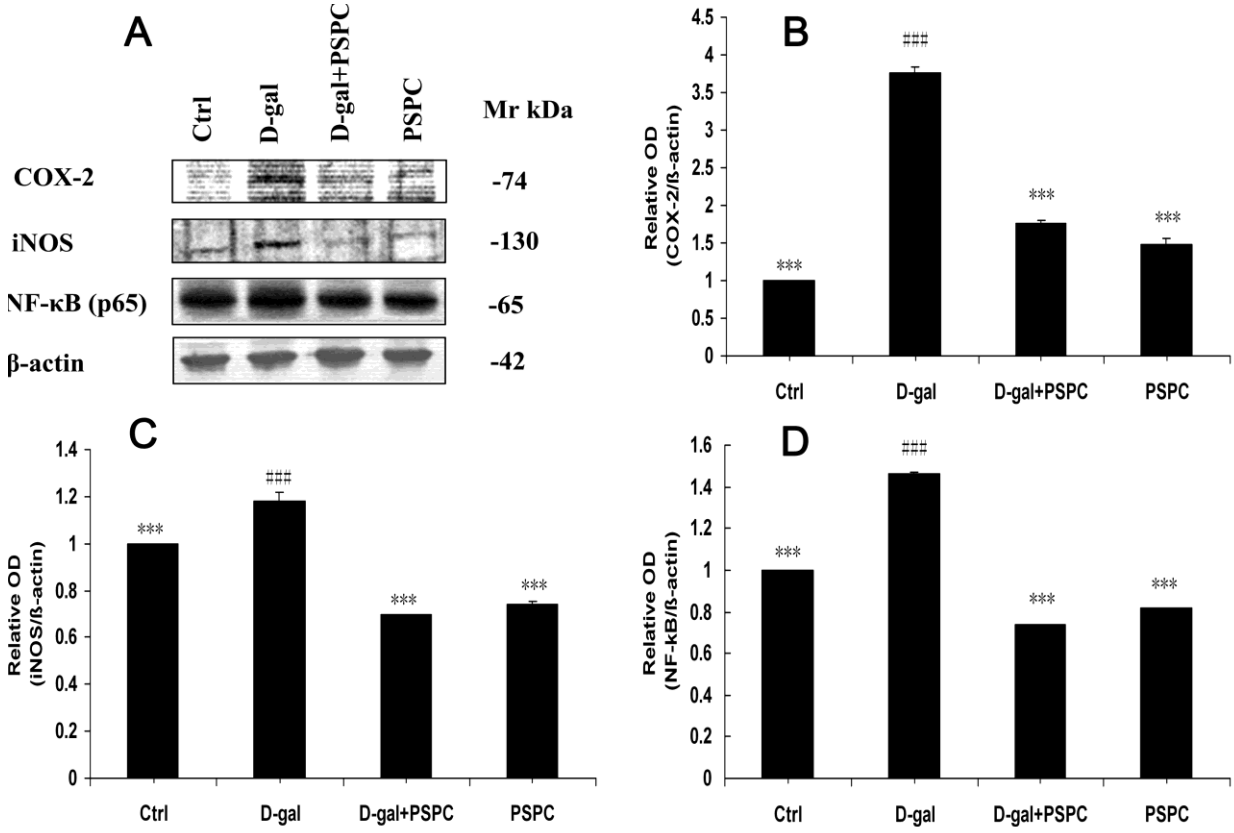

Figure 5. Western blot analysis of the COX-2, iNOS and NF-κB p65. (A) The effect of PSPC on the expression of COX-2, iNOS and NF-κB p65 in the kidneys of D-gal-treated mice. (B) Relative density analysis of the COX-2 protein bands. (C) Relative density analysis of the iNOS protein bands. (D) Relative density of the NF-κB p65 bands. β-Actin was probed as an internal control. The relative density is expressed as COX-2/β-actin, iNOS/β-actin or NF-κB/β-actin ratio and the vehicle control is set as 1.0. Values are averages from three independent experiments. Each value is the means ± S.E.M. ***P < 0.001, as compared to the D-gal model; # # #P < 0.001, as compared to the control group.

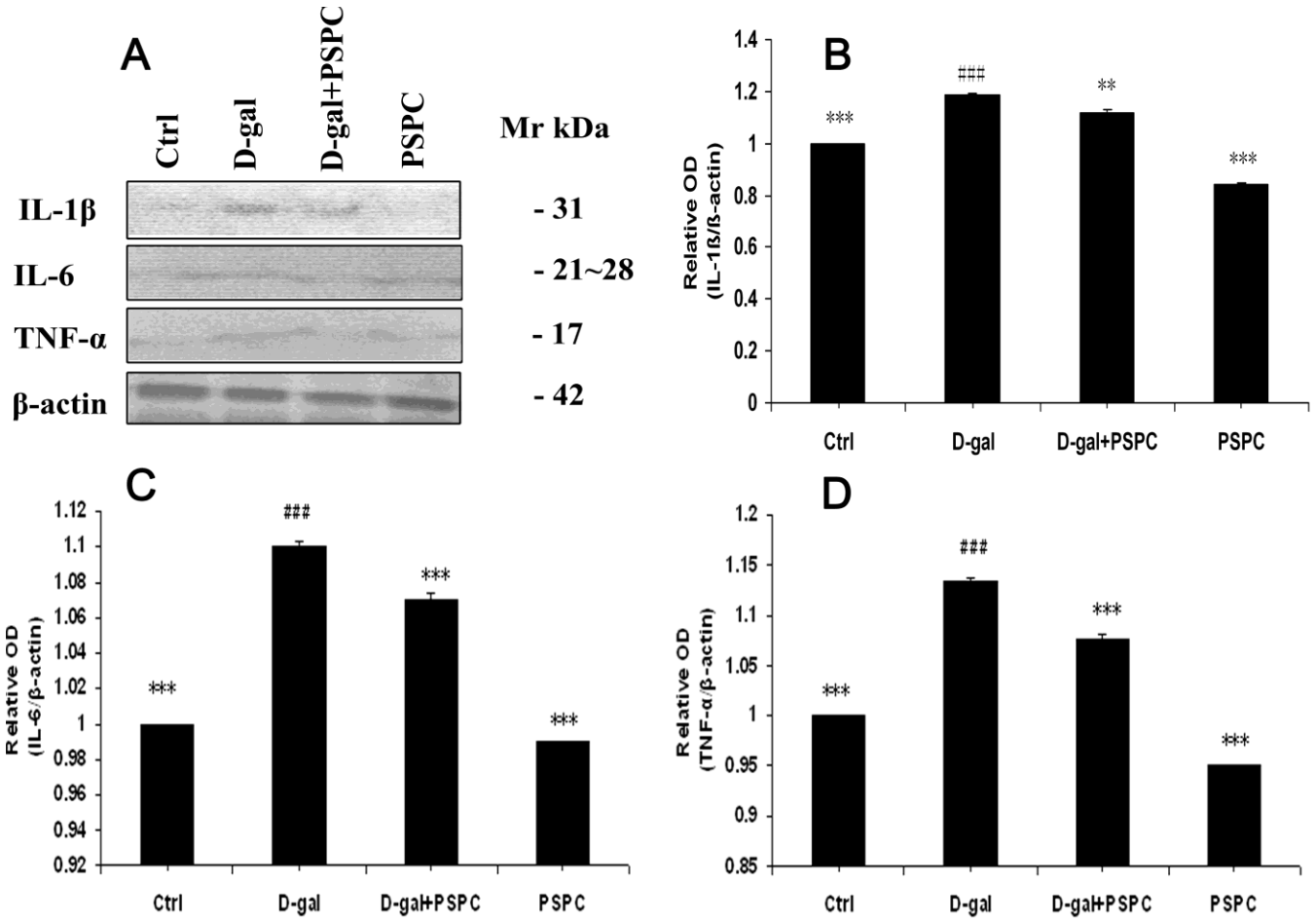

Figure 6. Western blot analysis of the IL-1β, IL-6 and TNF-α. (A) The effect of PSPC on the expression of IL-1β, IL-6 and TNF-α in the kidneys of D-gal-treated mice. (B) Relative density analysis of the IL-1β protein bands. (C) Relative density analysis of the IL-6 protein bands. (D) Relative density of the TNF-α bands. β-Actin was probed as an internal control. The relative density is expressed as IL-1β/β-actin, IL-6/β-actin or TNF-α/β-actin ratio and the vehicle control is set as 1.0. Values are averages from three independent experiments. Each value is the means ± S.E.M. ***P* < 0.01, ****P* < 0.001, as compared to the D-gal model; # # #*P* < 0.001, as compared to the control group.

shown in Figure 5, the semi-quantification of iNOS and COX-2 levels revealed a 10.0 and 276.3% increase,respectively, caused by treatment with D-gal (iNOS: *P* < 0.001; COX-2: *P* < 0.001). While, PSPC was shown to markedly inhibit the expressions of these molecules in the kidneys of D-gal-treated mice. Upon co-treatment with the PSPC, the intensities of the iNOS (P < 0.001) and COX-2 (P < 0.001) bands markedly reduced compared to D-gal treatment alone (Figure 5A, lane 3).

NF-κB is known to play a critical role in the regulation of genes involved in cell survival, and in the coordination of the expressions of pro-inflammatory enzymes including iNOS, COX-2 (Park et al., 2007). Therefore, we examined the levels of NF-κB p65 by Western blotting. After treatment with D-gal, the DNA-binding activity of NF-κB p65 in nuclear extract fractions increased by 0.5-fold (P < 0.001), compared to control (Figure 5A, lane 2). However, this binding activity decreased by 50.0% (P < 0.001) upon the presence of PSPC, compared to D-gal alone (Figure 5A, lane 3). Interestingly, no visible expression changes of iNOS, COX-2 and NF-κB p65 were seen in the kidneys from the mice treated with PSPC only, as compared with the controls.

Effects of PSPC on the expression of pro-inflammatory cytokines in the kidneys of D-gal-treated mice

IL-1β, IL-6 and TNF-α are known to be pro-inflammatory cytokines that possess a multitude of biological activities linked to the immune-pathology of inflammatory diseases (Moon et al., 2007). As shown in Figure 6, after treatment with D-gal, the expression of IL-1β, IL-6 and TNF-α were markedly increased (IL-1β: *P* < 0.001; IL-6: *P* < 0.001; TNF-α: *P* < 0.001). After D-gal stimulation with PSPC

treatment, the secretion of IL-1β, IL-6 and TNF-α were significantly decreased than that in single D-gal stimulation (IL-1β: $P < 0.01$; IL-6: $P < 0.001$; TNF-α: $P < 0.001$).

Interestingly, no visible expression changes of IL-1β, IL-6 and TNF-α were seen in the kidneys from the mice treated with PSPC only, as compared with the controls.

DISCUSSION

It has been suggested that several mechanisms may lead to the renal injury; one of the mechanisms involved is oxidative stress (Maldonado et al., 2003). Lipid peroxidation, a marker of oxidative stress is an autocatalytic, free radical mediated, destructive process, wherein polyunsaturated fatty acids in cell membranes undergo degradation to form lipid hydro peroxides (Kalayarasan et al., 2008). In our study, the increased levels of lipid peroxides in D-gal injured mice might be due to free radical mediated oxidative damage and the reflection of decrease in enzymic and nonenzymic antioxidants defense systems. Treatment with PSPC significantly decreased the levels of MDA in D-gal-injured mice. The free radical inhibitory activity of PSPC might be attributed to its antioxidant property and our data is consistent with previous reports (Zhang et al., 2009). Endogenous antioxidant enzymes (SOD, CAT and GPx) are responsible for the detoxification of deleterious oxygen radicals (Kalayarasan et al., 2008). In the present study, the decrease in the activities of SOD, CAT and GPx in the kidney of D-gal injured mice might be due to the increased production of free radicals and subsequent increase in lipid peroxidation (Iraz et al., 2006). The normalization of the antioxidant status during PSPC treatment could be due to the suppression of lipid peroxidation.

Inflammation is one of the leading causes of the many pathological states associated with oxidative stress (Dikalov et al., 2002). Inflammation is a complex response of the immune system to a pathogen (Luo et al., 2009). Although, it plays an important role in the immune defense, it also contributes to the pathogenesis mediated by oxidative stress (Rangasamy et al., 2005). Immune injury to the kidney is well documented (Halliwell and Gutteridge, 1990). In the current study, we furthermore investigated the core molecules involved in the pathway of inflammation. NO, a highly diffusible and short lived free radical gas has both physiological and pathological functions in many mammalian tissues (Kalayarasan et al., 2009). Excessive amounts of NO seem to cause damage when it combines with superoxide to form peroxynitrite ($ONOO^-$), a powerful oxidant that can be cleaved into highly reactive free radicals such as OH^- and NO_2^+. It is the overproduction of NO, not NO per se, that leads to cellular damage. In fact, NO at appropriate levels is critical for normal tissue homeostasis (Kiang et al., 2008; Oskoueian et al., 2011). NO is produced by a family of isozymes termed NO synthase (NOS). Among the three isoforms, inducible NOS (iNOS) is expressed in response to immunological stimuli. The different activators or inhibitors have been shown to induce, enhance or inhibit iNOS expression by different signaling pathways. However, in general, it seems that activation or inhibition of NF-κB pathway is one of the central mechanisms explaining the effects of many different regulators (Kleinert et al., 2004). Increased generation of NO is known to activate COX, which in turn converts arachidonic acid to prostaglandins. COX exists in two isoforms, the constitutive, COX-1 and inducible, COX-2 and is produced in abundance by activated macrophages and other cells at the site of inflammation (Sarkar et al., 2008). In this study, we first evaluated whether PSPC could regulate NO production and iNOS expression in the kidney of D-gal injured mice. The results of this study showed that PSPC could down-regulate D-gal-induced NO production (Figure 4) and iNOS expression (Figure 5C). Furthermore, the anti-inflammatory potential of PSPC was further corroborated by the concomitant decrease in expression of COX-2 (Figure 5B).

Expression of iNOS and COX-2 is largely regulated by transcriptional activation. Among these transcription factors, NF-κB, which is a primary transcription factor, is important in the inflammation (Inês et al., 2009). NF-κB is a key factor for regulating the expression of inflammation-associated enzymes and cytokine genes, such as iNOS, COX-2, TNF-α, IL-6 and IL-1β, which contain NF-κB-binding motifs within their respective promoters (Burk et al., 2010; Na et al., 2006). Under basal conditions, NF-κB is inactive and prevented from DNA binding and nuclear translocation by tight association in the cytoplasm with inhibitory proteins (Dinkova-Kostova et al., 2005). In our study, after treatment with D-gal, the expression of NF-κB p65 in nuclear extract fractions increased compared to control (Figure 5D). However, this binding activity decreased upon the presence of PSPC, compared to D-gal alone (Figure 5A, lane 3).

The proinflammatory cytokines such as TNF-α, IL-1β and IL-6 are small secreted proteins, which mediate and regulate inflammation. TNF-α induces a number of physiological effects including inflammation, septic shock, and cytotoxicity. IL-1β is one of the most important inflammatory cytokines secreted by macrophages, leading to cell or tissue damage during inflammatory process (Yun et al., 2008). Moreover, IL-6 is a cytokine that can facilitate autoimmune phenomena, amplify acute inflammation and promote the evolution into a chronic inflammatory state. It has a pivotal role in the systemic features of inflammation (Fonseca et al., 1990). Here, we evaluated whether PSPC regulate TNF-α, IL-1β and IL-6 expression in the kidney of D-gal injured mice. The results of this study showed that PSPC could down-regulate D-gal-induced TNF-α, IL-1β and IL-6 expression (Figure 6).

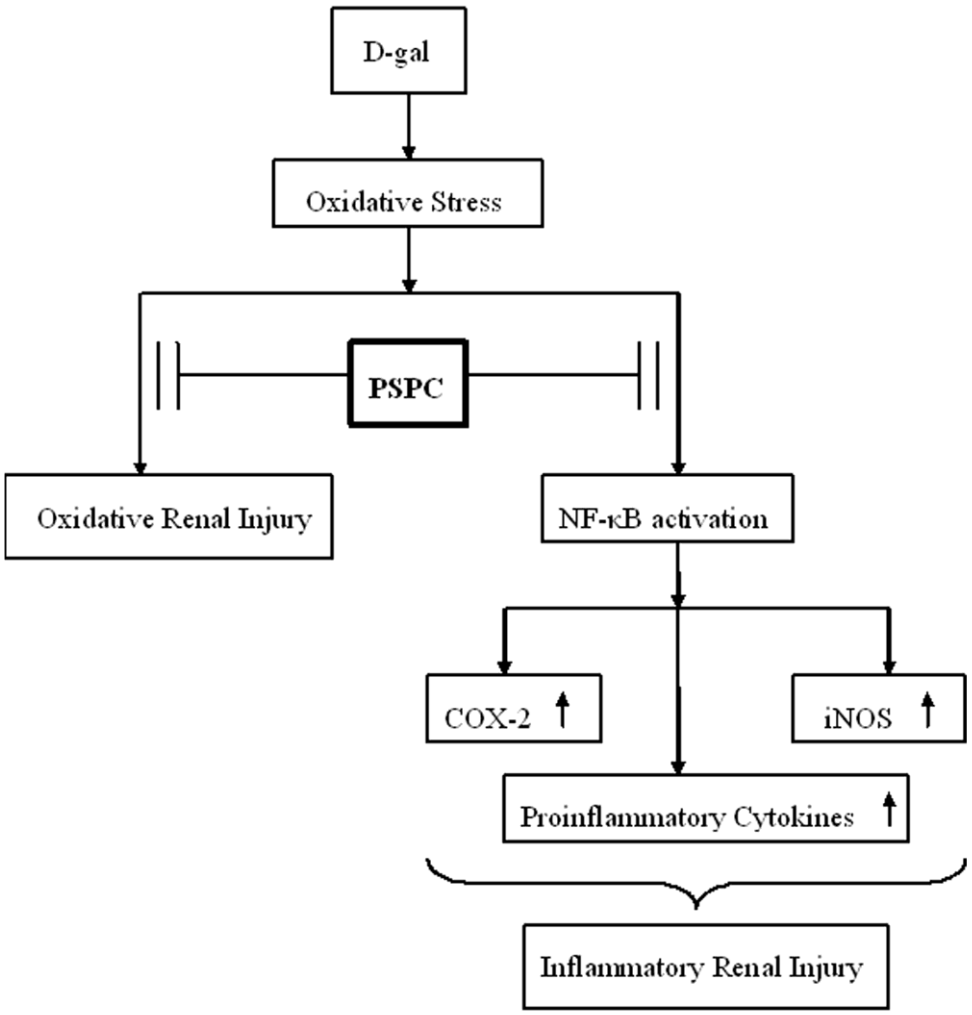

Figure 7. Schematic illustrating proposed mechanism by which PSPC prevents inflammatory renal injury. Treatment with D-gal causes increased oxidative stress. This results, in turn, in the activation of multiple NF-κB-responsive genes including proinflammatory cytokines, COX-2, and iNOS. PSPC inhibits lipid peroxidation and the activation of the above NF-κB-responsive genes, thereby protecting against inflammatory renal injury.

In conclusion, in the present study, we showed that PSPC, a class of naturally occurring anthocyanins used to color food (E163), was highly effective in attenuating D-gal-induced renal injury in mice. PSPC blocked lipid peroxidation, the activation of NF-κB, and the expression of proinflammatory cytokines, iNOS and COX-2 (Figure 7). Therefore, these results suggested that PSPC might be a potent therapeutic agent for renal injury with a broad spectrum of therapeutic mechanisms.

ACKNOWLEDGEMENTS

This work was supported by the Priority Academic Program Development of Jiangsu Higher Education Institutions (PAPD), the 2010 "Qinglan Project" of the Scientific and Technological Innovation Team Training Program of Jiangsu College and University, the National Natural Science Foundation of China (81171012; 30950031), the Major Fundamental Research Program of the Jiangsu Higher Education Institutions of China (07KJA36029), grants from the Natural Science Foundation for Colleges and Universities in Jiangsu Province (09KJB180009), grants from the Key Laboratory of Jiangsu Province, PR, China and grants from the Natural Science Foundation of Xuzhou Normal University (08XLR09, 09XLY05, 09XKXK02, 10XLA05).

REFERENCES

Aebi H (1984). Catalase *in vitro*. Methods Enzymol., 105: 121-126.
Burk DR, Cichacz ZA, Daskalova SM (2010). Aqueous extract of

Achillea millefolium L. (Asteraceae) inflorescences suppresses lipopolysaccharide-induced inflammatory responses in RAW 264.7 murine macrophages. J. Med. Plants Res., 3(4): 225-234.
Choi JH, Choi CY, Lee KJ, Hwang YP, Chung YC, Jeong HG (2009). Hepatoprotective effects of an anthocyanin fraction from purple-fleshed sweet potato against acetaminophen-induced liver damage in mice. J. Med. Food, 12(2): 320-326.
Dikalov SI, Dikalova AE, Mason RP (2002). Noninvasive diagnostic tool for inflammation-induced oxidative stress using electron spin resonance spectroscopy and an extracellular cyclic hydroxylamine. Arch. Biochem. Biophys., 402(2): 218-226.
Dinkova-Kostova AT, Liby KT, Stephenson KK, Holtzclaw WD, Gao X, Suh N, Williams C, Risingsong R, Honda T, Gribble GW, Sporn MB, Talalay P (2005). Extremely potent triterpenoid inducers of the phase 2 response: Correlations of protection against oxidant and inflammatory stress. Proc. Natl. Acad. Sci. USA., 102(12): 4584-4589.
Fan SH, Zhang ZF, Zheng YL, Lu J, Wu DM, Shan Q, Hu B, Wang YY (2009). Troxerutin protects the mouse kidney from D-galactose-caused injury through anti-inflammation and anti-oxidation. Int. Immunopharmacol., 9(1): 91-96.
Fonseca JE, Santos MJ, Canhão H, Choy E (1990). Interleukin-6 as a key player in systemic inflammation and joint destruction. Autoimmun. Rev., 8(7): 538-542.
Halliwell B, Gutteridge JM (1990). Role of free radicals and catalytic metal ions in human disease: an overview. Method Enzymol., 186: 1-85.
Hua X, Lei M, Zhang Y, Ding J, Han Q, Hu G, Xiao M (2007). Long-term D-galactose injection combined with ovariectomy serves as a new rodent model for Alzheimer's disease. Life Sci., 80(20): 1897-1905.
Inês AM, Rocha J, Vila-Real H, Eduardo-Figueira M, Mota-Filipe H, Sepodes B, Ribeiro MH (2009). Anti-inflammatory activity of naringin and the biosynthesised naringenin by naringinase immobilized in microstructured materials in a model of DSS-induced colitis in mice. Food Res. Int., 42(8): 1010-1017.
Iraz M, Ozerol E, Gulec M, Tasdemir S, Idiz N, Fadillioglu E, Naziroglu M, Akyol O (2006). Protective effect of caffeic acid phenethyl ester (CAPE) administration on cisplatin-induced oxidative damage to liver in rat. Cell Biochem. Funct., 24(4): 357-361.
Kalayarasan S, Prabhu PN, Sriram N, Manikandan R, Arumugam M, Sudhandiran G (2009). Diallyl sulfide enhances antioxidants and inhibits inflammation through the activation of Nrf2 against gentamicin-induced nephrotoxicity in Wistar rats. Eur. J. Pharmacol., 606(1-3): 162-171.
Kalayarasan S, Sriram N, Sudhandiran G (2008). Diallyl sulfide attenuates bleomycin-induced pulmonary fibrosis: Critical role of iNOS, NF-κB, TNF-α and IL-1β. Life Sci., 82(23-24): 1142-1153.
Kiang JG, Krishnan S, Lu X, Li Y (2008). Inhibition of inducible nitric-oxide synthase protects human T cells from hypoxia-induced apoptosis. Mol. Pharmacol., 73(3): 738-747.
Kim HY, Okamoto T, Yokozawa T (2009). Beneficial effects of Chinese prescription Kangen-karyu on diabetes associated with hyperlipidemia, advanced glycation endproducts, and oxidative stress in streptozotocin-induced diabetic rats. J. Ethnopharmacol., 124(2): 263-269.
Kleinert H, Pautz A, Linker K, Schwarz PM (2004). Regulation of the expression of inducible nitric oxide synthase. Eur. J. Pharmacol., 500(1-3): 255-266.
Li L, Ng TB, Gao W, Li W, Fu M, Niu SM, Zhao L, Chen RR, Liu F (2005). Antioxidant activity of gallic acid from rose flowers in senescence accelerated mice. Life Sci., 77(2): 230-240.
Lu J, Zheng YL, Luo L, Wu DM, Sun DX, Feng YJ (2005). Quercetin reverses D-galactose induced neurotoxicity in mouse brain. Behav. Brain Res., 171(2): 251-260.
Lu J, Zheng YL, Wu DM, Luo L, Sun DX, Shan Q (2007). Ursolic acid ameliorates cognition deficits and attenuates oxidative damage in the brain of senescent mice induced by D-galactose. Biochem. Pharmacol., 74(7): 1078-1090.
Luo L, Wang Y , Feng Q, Zhang H, Xue B, Shen J, Ye Y, Han X, Ma H, Xu J, Chen D, Yin Z (2009). Recombinant protein glutathione *S*-transferases P1 attenuates inflammation in mice. Mol. Immunol., 46(5): 848-857.
Maldonado PD, Barrera D, Rivero I, Mata R, Medina-Campos ON, Hernández-Pando R, Pedraza-Chaverrí J (2003). Antioxidant S-allylcysteine prevents gentamicin-induced oxidative stress and renal damage. Free Radic. Biol. Med., 35(3): 317-324.
Matsui T, Ebuchi S, Kobayashi M, Fukui K, Sugita K, Terahara N, Matsumoto K (2002). Anti-hyperglycemic effect of diacylated anthocyanin derived from *Ipomoea batatas* cultivar Ayamurasaki can be achieved through the alpha-glucosidase inhibitory action. J. Agric. Food Chem., 50(25): 7244-7248.
Mihara M, Uchiyama M (1978). Determination of malonaldehyde precursor in tissues by thiobarbituric acid test. Anal. Biochem., 86(1): 271-278.
Miyazaki K, Makino K, Iwadate E, Deguchi Y, Ishikawa F (2008). Anthocyanins from purple sweet potato *Ipomoea batatas* cultivar Ayamurasaki suppress the development of atherosclerotic lesions and both enhancements of oxidative stress and soluble vascular cell adhesion molecule-1 in apolipoprotein E-deficient mice. J. Agric. Food Chem., 56(23): 11485-11492.
Moon DO, Park SY, Lee KJ, Heo MS, Kim KC, Kim MO, Lee JD, Choi YH, Kim GY (2007). Bee venom and melittin reduce proinflammatory mediators in lipopolysaccharide-stimulated BV2 microglia. Int. Immunopharmacol., 7(8): 1092-1101.
Mulabagal V, Lang GA, DeWitt DL, Dalavoy SS, Nair MG (2009). Anthocyanin content, lipid peroxidation and cyclooxygenase enzyme inhibitory activities of sweet and sour cherries. J. Agric. Food Chem., 57(4): 1239-1246.
Na HJ, Lee G, Oh HY, Jeon KS, Kwon HJ, Ha KS, Lee H, Kwon YG, Kim YM (2006). 4-*O*-Methylgallic acid suppresses inflammation-associated gene expression by inhibition of redox-based NF-κB activation. Int. Immunopharmacol., 6(10): 1597-1608.
Oskoueian E, Abdullah N, Saad WZ, Omar AR, Ahmad S, Kuan WB, Zolkifli NA, Hendra R, Ho YW (2011). Antioxidant, anti-inflammatory and anticancer activities of methanolic extracts from *Jatropha curcas* Linn. J. Med. Plants Res., 5(1): 49-57.
Paglia DE, Valentine WN (1967). Studies on the quantitative and qualitative characterization of erythrocyte glutathione peroxidase. J. Lab. Clin. Med., 70(1): 158-169.
Park HJ, Kim IT, Won JH, Jeong SH, Park EY, Nam JH, Choi T, Lee KT (2007). Anti-inflammatory activities of *ent*-16α*H*, 17-hydroxy-kauran-19-oic acid isolated from the roots of *Siegesbeckia pubescens* are due to the inhibition of iNOS and COX-2 expression in RAW 264.7 macrophages via NF-κB inactivation. Eur. J. Pharmacol., 558(1-3): 185-193.
Peteros NP, Uy MM (2010). Antioxidant and cytotoxic activities and phytochemical screening of four Philippine medicinal plants. J. Med. Plants Res., 4(5): 407-414.
Piccolella S, Fiorentino A, Pacifico S, D'Abrosca B, Uzzo P, Monaco P (2008). Antioxidant properties of sour cherries (*Prunus cerasus* L.): role of colorless phytochemicals from the methanolic extract of ripe fruits. J. Agric. Food Chem., 56(6): 1928-1935.
Qiu F, Luo J, Yao S, Ma L, Kong L (2009). Preparative isolation and purification of anthocyanins from purple sweet potato by high-speed counter-current chromatography. J. Sep. Sci., 32(12): 2146-2151.
Rangasamy T, Guo J, Mitzner WA, Roman J, Singh A, Fryer AD, Yamamoto M, Kensler TW, Tuder, RM, Georas SN, Biswal S (2005). Disruption of *Nrf2* enhances susceptibility to severe airway inflammation and asthma in mice. J. Exp. Med., 202(1): 47-59.
Sakatani M, Suda I, Oki T, Kobayashi S, Kobayashi S, Takahashi M (2007). Effects of purple sweet potato anthocyanins on development and intracellular redox status of bovine preimplantation embryos exposed to heat shock. J. Reprod. Develop., 53(3): 605-614.
Sarkar D, Saha P, Gamre S, Bhattacharjee S, Hariharan C, Ganguly S, Sen R, Mandal G, Chattopadhyay S, Majumdar S, Chatterjee M (2008). Anti-inflammatory effect of allylpyrocatechol in LPS-induced macrophages is mediated by suppression of iNOS and COX-2 via the NF-κB pathway. Int. Immunopharmacol., 8(9): 1264-1271.
Shih PH, Yeh CT, Yen GC (2005). Effects of anthocyanidin on the inhibition of proliferation and induction of apoptosis in human gastric adenocarcinoma cells. Food Chem. Toxicol., 43(10): 1557-1566.
Wu DM, Lu J, Zheng YL, Zhou Z, Shan Q, Ma DF (2008). Purple sweet potato color repairs D-galactose-induced spatial learning and memory impairment by regulating the expression of synaptic proteins.

Neurobiol. Learn. Mem., 90(1): 19-27.
Yoshimoto M, Okuno S, Yamaguchi M, Yamakawa O (2001). Antimutagenicity of deacylated anthocyanins in purple-fleshed sweetpotato. Biosci. Biotechnol. Biochem., 65(7): 1652-1655.
Yun KJ, Koh DJ, Kim SH, Park SJ, Ryu JH, Kim DG, Lee JY, Lee KT (2008). Anti-inflammatory effects of sinapic acid through the suppression of inducible nitric oxide synthase, cyclooxygase-2, and proinflammatory cytokines expressions via nuclear factor-κB inactivation. J. Agric. Food Chem., 56(21): 10265-10272.
Zhang Q, Li X, Cui X, Zuo P (2005). D-galactose injured neurogenesis in the hippocampus of adult mice. Neurol. Res., 27(5): 552-556.
Zhang ZF, Fan SH, Zheng YL, Lu J, Wu DM, Shan Q, Hu B (2009). Purple sweet potato color attenuates oxidative stress and inflammatory response induced by D-galactose in mouse liver. Food Chem. Toxicol., 47(2): 496-501.